Video Article

Fabrication of Superhydrophobic Metal Surfaces for Anti-Icing Applications

F.J. Montes Ruiz-Cabello[1], Pablo Ibañez-Ibañez[1], Guillermo Paz-Gomez[1], Miguel Cabrerizo-Vilchez[1], Miguel Angel Rodriguez-Valverde[1]

[1]Biocolloid and Fluid Physics Group, Faculty of Sciences, Applied Physics Department, University of Granada

Correspondence to: F.J. Montes Ruiz-Cabello at fjmontes@ugr.es

URL: https://www.jove.com/video/57635
DOI: doi:10.3791/57635

Keywords: Engineering, Issue 138, Superhydrophobic metal surfaces, durability, anti-icing, acid etching, silanization, ice adhesion, freezing delay

Date Published: 8/15/2018

Citation: Montes Ruiz-Cabello, F., Ibañez-Ibañez, P., Paz-Gomez, G., Cabrerizo-Vilchez, M., Rodriguez-Valverde, M.A. Fabrication of Superhydrophobic Metal Surfaces for Anti-Icing Applications. *J. Vis. Exp.* (138), e57635, doi:10.3791/57635 (2018).

Abstract

Several ways to produce superhydrophobic metal surfaces are presented in this work. Aluminum was chosen as the metal substrate due to its wide use in industry. The wettability of the produced surface was analyzed by bouncing drop experiments and the topography was analyzed by confocal microscopy. In addition, we show various methodologies to measure its durability and anti-icing properties. Superhydrophobic surfaces hold a special texture that must be preserved to keep their water-repellency. To fabricate durable surfaces, we followed two strategies to incorporate a resistant texture. The first strategy is a direct incorporation of roughness to the metal substrate by acid etching. After this surface texturization, the surface energy was decreased by silanization or fluoropolymer deposition. The second strategy is the growth of a ceria layer (after surface texturization) that should enhance the surface hardness and corrosion resistance. The surface energy was decreased with a stearic acid film.

The durability of the superhydrophobic surfaces was examined by a particle impact test, mechanical wear by lateral abrasion, and UV-ozone resistance. The anti-icing properties were explored by studying the ability to repeal subcooled water, freezing delay, and ice adhesion.

Video Link

The video component of this article can be found at https://www.jove.com/video/57635/

Introduction

The ability of superhydrophobic (SH) surfaces to repel water is the reason that they are traditionally proposed as a solution to prevent icing[1,2]. However, there are concerns about the suitability of SH surfaces for anti-icing agents: 1) the high costs of production, 2) that superhydrophobicity does not always lead to ice-phobicity[3], and 3) the questionable durability of the SH surfaces[4]. Superhydrophobic surfaces hold two properties related to their topography and chemical composition[5]: they are rough, with particular topographic features; and their surface energy is low (intrinsically hydrophobic).

The roughness on a hydrophobic surface serves to reduce the ratio between the real solid-liquid area and the apparent contact area. The water is not fully in contact with the solid due to the lotus effect[6,7], when the drop rests or moves onto the surface asperities. In this scenario, the solid-liquid interface acts heterogeneously with two chemical domains: the solid surface itself and the tiny air-bubbles trapped between the solid and water[8]. The degree of water repellency is connected to the amount of trapped air because the air patches are smooth and its intrinsic contact angle is 180°. Some studies report the incorporation of a hierarchical surface texture with micro and nano-asperities as the optimal strategy to provide better water-repellent properties (greater presence of air at the solid-liquid interface)[9]. For some metals, a low-cost strategy to create two-level roughness features is acid-etching[10,11]. This procedure is frequently used in industry. With certain acid concentrations and etching times, the metal surface reveals the proper hierarchical roughness. In general, the surface roughening is optimized by varying the acid concentration, etching time, or both[12]. The surface energy of metals is high and for this reason, the fabrication of water-repellent metal surfaces requires later hydrophobization.

Hydrophobization is generally achieved by hydrophobic film deposition using different methods: silanization[10,13], dip-coating[14], spin-coating[15], spraying[16] or plasma-deposition[17]. Silanization has been proposed[18] as one of the most promising tool for improving the low durability of SH surfaces. Unlike other deposition techniques, the silanization process is based on a covalent bond between the Si-OH groups with the surface hydroxyl groups of the metal substrate[10]. A drawback of the silanization process is the need for previous activation of the metal substrate to create enough hydroxyl groups for a high degree of coverage and uniformity. Another strategy recently proposed to produce resistant superhydrophobic surfaces is the use of rare-earth coatings[19,20]. Ceria coatings have two properties that justify this use: they can be intrinsically hydrophobic[21], and they are mechanically and chemically robust. In particular, one of the most important reasons why they are chosen as protective coatings is their corrosion-protection abilities[20].

To produce long-lasting SH metal surfaces, two issues are considered: the surface texture must not be damaged, and the hydrophobic film/coating must be firmly anchored to the substrate. Surfaces are typically exposed to wear originated by lateral abrasion or particle impact[4]. If the asperities are damaged, the water-repellency may be substantially reduced. Under extreme environments, the hydrophobic coating may be

partially removed from the surface or may be chemically degraded by UV exposure, humidity or corrosion. The design of durable SH surfaces coatings is an important challenge for coating and surface engineering.

For metals, one of the most demanding requirements is that the anti-icing ability is based on three interconnected aspects[22] as illustrated in **Figure 1**: subcooled water repellency, freezing delay, and low ice-adhesion. Outdoor icing occurs when subcooled water, typically rain drops, comes into contact with a solid surface and is rapidly frozen by heterogeneous nucleation[23]. The formed ice (rime) is firmly attached to the surface. Thus, the first step to avoid icing is to reduce the solid-water contact time. If the surface is superhydrophobic, rain drops may be expelled from the surface before freezing. In addition, it has been proven that, under humid conditions, surfaces with a high contact angle delay freezing more efficiently than those ones with a low contact angle[24]. For these two reasons, SH surfaces are the most appropriate surfaces to mitigate icing. However, the lifetime of superhydrophobic surfaces may be a key point since icing conditions are typically aggressive[25]. Some studies have concluded that SH surfaces are not the best choice for decreasing ice adhesion[26]. Once the ice forms on the surface, it stays firmly attached due to surface asperities. The roughness increases the ice-surface contact area and the asperities act as interlocking agents[26]. The use of durable SH surfaces is recommended to avoid icing if there are no traces of ice already present on the surface.

In this work, we present several protocols to produce durable SH surfaces on metal substrates. We use aluminum (Al) as the substrate because it is widely used in industry, and the incorporation of anti-icing properties is particularly relevant for certain applications (ski resorts facilities, aeronautics, *etc.*). We prepare three types of surfaces: a textured Al surface coated with a fluoropolymer coating, a textured Al surface silanized with a fluorosilane, and a ceria-stearic acid bilayer on an Al substrate. Similar techniques[17,27,28,29] provide 100-300 nm film thicknesses or even monolayer films. For each surface, we measured their wetting properties and conducted wear tests. Finally, we analyzed their anti-icing performance by using three tests aimed to probe independently the three properties shown in **Figure 1**.

Our protocol is based on the scheme shown in **Figure 2**. Once the SH Al surfaces are prepared, their wetting properties and topography are analyzed to determine their repellency properties and roughness features. The wetting properties are analyzed by bouncing drop experiments, which is a technique connected to the water tensile adhesion. Since the observation of drop bounces is required, this technique is only suitable for superhydrophobic surfaces[13]. For each surface treatment, we prepared at least four samples to conduct the anti-icing tests and another four samples to perform the durability tests. The damage caused after each durability test was analyzed by measuring the loss of wetting properties and roughness features. Similar durability tests to the proposed ones in this work were recently used for other metal surfaces[27,30].

Concerning the anti-icing tests, the aim of this study is to determine whether the use of the produced SH Al surfaces are convenient as anti-icing agents. Hence, we analyzed, for comparison, the performance of two control samples: a) an untreated Al sample (smooth hydrophilic sample) and b) a hydrophobized but not textured sample (smooth hydrophobic sample). For the same purpose, the use of a textured but not hydrophobized surface might be of interest. Unfortunately, this surface is extremely wettable and anti-icing tests cannot be carried out for them.

Protocol

Note: The protocol follows the scheme shown in **Figure 2**.

1. Sample Preparation

1. **Cutting and cleaning**
    1. Using a metal shear, cut 250 mm x 250 mm x 0.5 mm sheets of aluminum into 25 mm x 45 mm x 0.5 mm pieces.
    Note: Special care must be taken when using the metal shear, and special training may be necessary.
    2. Remove the protective film covering one side of the sample and wash this side using around 50 mL of cleaning solution. Wash the samples gently with gloved hands. Avoid the use of abrasive scourers.
    3. Rinse the samples abundantly in a flow of distilled water. Subsequently, immerse each sample in 30 mL of 96% ethanol, sonicate it for 300 s, and repeat in 30 mL of ultrapure water for 300 s.
    4. Remove the samples from the water and dry them for 1 h at room temperature.

2. **Acid etching**
    1. For the etching reaction, prepare a 4 M solution of HCl in ultrapure water[13]. Immerse each sample in 80 mL of this solution for 480 s. The reaction becomes more vigorous after approximately 360 s, when the native oxide surface layer is removed.
    CAUTION: For safety, conduct this reaction in a hood. Wear gloves, lab coat and protective glasses.
    2. Next to the beaker containing the acid solution, prepare another beaker with ultrapure water to abruptly stop the reaction. Using polytetrafluoroethylene tweezers, remove the sample from the acid solution and immerse it in water. Rinse the sample in abundant ultrapure water.
    3. Dry the samples completely by blowing them with filtered and compressed air. Note that the sample after the etching reaction is superhydrophilic and drying it may be a difficult task. After the macroscopic removal of water by blowing, remove traces of water in an oven at 120 °C for 600 s.
    Note: This drying process in essential, especially for samples to be later silanized.

3. **Hydrophobization**
    1. **Hydrophobization by FAS-17 silanization**
        1. Prior to the vapor-phase silanization, treat the samples with air-plasma for 600 s using a plasma cleaner operating at 100 W. This process activates the surface functional groups (-OH groups) that act as linker to the silane molecules.
        2. Subsequently, introduce the samples inside a glass Petri dish slightly tilted with the help of a pipette tip to slightly incline the surface. Deposit two 50 µL drops of 1H,1H,2H,2H-Perfluorodecyl-triethoxysilane (FAS-17) on the Petri dish next to the sample[13].
        3. Cover the Petri dish partially and place it in an air-evacuated desiccator overnight. Finally, ventilate the desiccator. Remove the samples, which are ready to use.

2. **Hydrophobization by fluoropolymer** (**polytetrafluoroethylene) deposition**
    1. Spray the etched samples[16] from about 10 cm with a solution of amorphous fluoropolymer in a fluorocarbon solvent in a ratio of 1/20 (v/v)[16]. A perfume diffuser filled with the solution may be used for this purpose. Leave to dry at room temperature for 600 s. Repeat the same process over a clean non-etched surface to make a smooth-hydrophobic aluminum surface (R_a = 0.25±0.03 µm).
    2. Apply a second coat and introduce the samples in a 110 °C oven for 600 s to ensure total removal of the solvent and a crosslinking of the fluoropolymer coating. This process increases the durability, as indicated by the manufacturer.

3. **Hydrophobization by ceria-stearic acid deposition**
    1. Clean the etched samples in acetone/ethanol/water, sonicate them for 300 s in water and dry them in a flow of compressed air.
    2. Immerse the samples[31] in 50 mL of aqueous solution containing 2 g of cerium trichloride heptahydrate ($CeCl_3 \cdot 7H_2O$), and 3 mL of 30% hydrogen peroxide (H_2O_2). Incubate the sample immersed in the solution in a 40 °C oven for 1 h.
    3. Remove it from the solution, rinse it in distilled water and dry it in a 100 °C oven for 600 s.
    4. Immerse the sample in a 30 mM ethanol solution of stearic acid for 900 s, rinse it in ethanol and dry it in a 100 °C oven for 600 s.
    Note: Once dried and cooled down to room temperature, the samples are ready to use. The SH surfaces produced with the ceria-stearic coating acid are hereinafter referred as the Ce-SA coated surface.

2. Sample Characterization

1. **Wetting analysis**
    1. **Bouncing drop experiments**
        1. Evaluate the water repellency degree of the produced sample by bouncing drops experiments[13]. Quantify the number of bounces given by a drop that is released from a fixed syringe whose needle is located at (10.1 ± 0.2) mm above the surface. The drop volume is typically 4 µL.
        2. Capture the sequence with a high-speed camera. In the high-speed video acquisition software, fix the acquisition rate to 4200 images per second and the exposure time to 235 µs.
        3. Once the video is recorded, select the sequence from the moment when the drop is released until the drop is already in full contact with the sample (no more bounces are observed). Save the video file.
        4. For each image, detect the drop profile using software[32]. Subsequently, quantify the number of bounces with the naked eye when playing the video sequence. In case that it is not easily identified, count the number of maxima above the center of mass position of the static drop (more than 15-20%).

    2. **Tilting plate experiments**
        1. Use this test only to quantify the damage caused by each specific wear test. Analyze the shear adhesion of water drops with tilting plate experiments (TPE)[33] using a lab-designed tilting apparatus[34].
        2. Use side-view image acquisition of a sessile drop deposited on the sample fixed to an inclinable platform. During the image acquisition (at constant acquisition rate of 16 fps), incline the platform with constant angular velocity (5°/s). Therefore, capture a drop image every 0.31°.
        Note: Above a specific inclination angle, the drop moves (slides/rolls-off) on the surface and this state may serve to determine the advancing and receding contact angles (ACA and RCA, respectively) simultaneously. The minimum tilting angle that produces a global displacement of the contact line (uphill and downhill contact line points move simultaneously) is referred to as the sliding angle (SA). The SA is the value reported here from TPE.

2. **Roughness measurements**
    1. Analyze the micro-roughness of the samples using a white light confocal microscope. Set a scanning area of 0.252 x 0.187 mm per single topography.
    2. Take at least 4 single topographies per sample. Use the objective of magnification 50X, capturing 200 vertical planes in vertical steps of 0.2 µm. Determine the Ra factor (arithmetic roughness amplitude).

3. Durability Tests

Note: Evaluate the damage induced by each wear agent separately. Do not conduct more than one wear test per sample.

1. **Lateral abrasion tests**
Note: The lateral abrasion tests (see **Figure 3a**) are performed by means of a commercial linear abrasive. This test aims to evaluate the wear induced by tangential displacement of a standard abrasive tip against a surface. This device allows the use of a wide variety of abrasives, setting a wide range of application pressures, lateral speeds and total number of abrasive cycles[35].
    1. Use a standard rubber abrasive CS-10, provided by the manufacturer. Fix the velocity to 20 cycles/min. Control the applied pressure by using weights. Set the minimum pressure allowed by the instrument, which corresponds to a total weight of 350 g.
    Note: Considering the tip width (6.70±0.05 mm), and the weight used, the corresponding applied pressure for these settings is 97.3±1.4 kPa. The total worn area is limited by the width of the tip and the total length for each abrasion cycle. Set it to 38.1 mm.
    2. For each sample, evaluate the wear induced after 1, 2, 3 and 5 cycles.
        1. After each wear treatment, gently brush the surface (using the brush provided by the manufacturer), rinse in water, and blow on using compressed air. Evaluate the wetting properties using TPE, as described in section 2.1.2.

2. **Abrasive particle impact test**
    1. Conduct the particle impact test by using the set-up shown in **Figure 3b**, which is inspired by the standard abrasion Test D968. Release 30 mL (around 55 g) of abrasive sand from a glass funnel. Locate its extreme bottom at (25±1) cm from the surface.
    2. Use a funnel tap diameter of (12±1) mm and a length of (97±1) mm. Place the funnel vertically, while inclining the sample 45°. After impacting on the sample, collect the sand in a container placed below.
    3. Once a wear cycle is conducted, rinse the surface with distilled water, dry it in a flow of compressed air and evaluate the wetting properties by TPE (section 2.1.2). Repeat this entire process up to 3 times for each sample.

3. **UV-ozone surface degradation test**
    1. Conduct the UV-ozone degradation test using an ozone cleaner. Treat each sample at room temperature for 600 s and repeat the cycle once.
    2. Subsequently, rinse the surfaces in water and dry them with compressed air.
    3. Evaluate the wetting properties by TPE described in section 2.1.2 to determine whether the superhydrophobic properties remain after UV-exposure.

4. **Water immersion test**
    1. Evaluate the wear induced by water contact after a lengthy immersion in water. Introduce the sample in a 100 mL beaker of ultrapure water for 24 h.
    2. Remove the samples from the water, dry them with compressed air and place them in a 120 °C oven for 600 s to ensure a total removal of water from the surface. When the surface is fully dried, evaluate the wetting properties after water exposure using the protocol described in section 2.1.2.

4. Anti-icing Efficiency Evaluation

Note: The anti-icing efficiency evaluation is based on the three aspects shown in **Figure 1**.

1. **Subcooled water dripping test**
   Note: The subcooled water repellency of the samples is tested by means of the set-up shown in **Figure 4a**. The sample is introduced inside a freezing chamber at –20 °C, which is fixed on top of an inclined (30°) platform. A mixture of ice and distilled water in equilibrium (at stabilized temperature of 0 °C) is placed outside the freezing chamber.
    1. Pump the cold water inside the chamber using a peristaltic pump and have it circulate inside the freezer before being dripped on the sample at a low rate of 1 drop every 3 seconds. Single drops have a volume of roughly 50 µL.
    2. Once the dripping process is initiated, capture a lateral image of the sample every 10 s to determine whether ice accretion occurs.

2. **Freezing delay test**
    1. Conduct the freezing delay test inside the same freezing chamber mentioned in the previous section.
    2. Determine the percentage of sessile drops deposited on the sample that freeze, for each temperature, during a cooling process from room temperature down to approximately -25 °C. The set-up for this test is shown in **Figure 4b**.
    3. Level the sample (with zero tilt) and deposit sessile drops carefully to avoid roll-off. Due to the high mobility of drops on water-repellent surfaces, place a lower number of them on SH samples. Repeat the experiment for SH surfaces several times.
    4. Monitor the temperature and relative humidity by using a thermal-probe. Control the relative humidity (RH) with a commercial humidifier. The RH is roughly 95% when the humidifier is switched on, and it decreases down to approximately 40% when the humidifier is switched off.
    5. Use around 200 drops of 30 µL per sample (drop freezing is a stochastic phenomenon, and the analysis requires the use of a large number of drops).
       Note: Thus, for this test use larger samples than those used for the rest of the studies. In this case the size is 125 mm x 62.5 mm and adapt the protocol to either etch the sample or hydrophobize their surfaces to the new sample dimensions.
    6. Place the sample in the middle of the bottom part of the freezer on top of an isolating platform. Gently deposit an array of 70 drops per sample (25 for the superhydrophobic sample). Close the freezer and turn it on.
       Note: The temperature decreases linearly in time from room temperature down to approximately -25 °C. The rate of cooling depends on the relative humidity. At low relative humidity (humidifier unplugged), the entire process takes roughly 2 hours, while it takes less time (around 1 hour) if the humidifier is connected. Once the temperature is lower than 0 °C, drops start to nucleate.
    7. Count the number of drops that are frozen for each temperature (in intervals of 0.5 °C), until all the totality of the drops is frozen.

3. **Ice adhesion test**
    1. Quantify the force that must be applied to detach (pull-off) a piece of ice with a controllable contact area that has been formed on each sample. Perform these tests using the set-up illustrated in **Figure 4c**.
    2. Cut a polytetrafluoroethylene pipe with internal diameter of 10 mm in cylinders of ~28 mm height using scissors. Press the cylinder against the sample. Fill it with 1.2 mL of distilled water. Introduce the filled cylinder in the freezing chamber and wait for 1 h.
       Note: Once the water is totally frozen, the sample with the cylinder is firmly fixed to a platform using a striker plate.
    3. Tie the cylinder to a digital force gauge using a nylon thread. The way this cylinder is tied to the thread and the orientation of the cylinder with respect to the thread depends on which type (shear or the tensile) adhesion is under evaluation. Fix this gauge to a motorized test stand. Close the freezing chamber and wait for 600 s.
    4. Displace the gauge from the sample at a constant velocity of (10 ± 0.5) mm/min.
        1. Adjust this velocity manually within the control panel of the motorized test stand. Click the icon of the program controlling the dynamometer readings. Press **START** to record the force.
        2. Immediately after, move the dynamometer upwards by keeping on pressing the vertical displacement bottom within the motorized stand control panel.

5. When the displacement of the dynamometer with respect to the sample produces an extension of the thread and a separation of the ice from the sample, click on **STOP** and save the generated data file.
   Note: The gauge monitors the force in terms of time. Knowing the velocity in which the dynamometer is displaced (10 mm/min), determine the force in terms of displacement. This serves to determine the rupture force (maximum retaining force) and the adhesion strength per unit area.
6. Evaluate the shear adhesion when the pull-off is carried out laterally. The force in this case is parallel applied to the contact area (see **Figure 4b**). For this purpose, fix the sample vertically and connect the cylinder base to the thread using a metal ring. Pull this ring by the gauge until the sample detaches from the surface by shear displacement.
   Note: The tensile adhesion test evaluates the peak force and work need to detach a piece of ice from the surface when it is pulled vertically.
7. In this case, drill two small holes on the cylinder wall that serve to connect the cylinder to the gauge. Then, pull it vertically until the ice is finally detached from the surface.

Representative Results

The wetting and roughness properties of the SH surfaces that were used in this study are shown in **Figure 5**. The average number of bounces measured for each sample is displayed in **Figure 5a** and the average roughness is shown in **Figure 5b**. There is no correlation between the roughness and wetting properties. The number of bounces measured for the polytetrafluoroethylene coated sample agrees with the Ce-SA sample. However, the Ce-SA sample is clearly rougher (~40% greater Ra value). In contrast, the Ra value for the FAS-17 sample is very similar to the polytetrafluoroethylene, while their wetting properties are clearly different.

In **Figure 6** we analyzed the effect on the wetting properties of three durability tests: the lateral abrasion test (**Figure 6a**), the particle impact test (**Figure 6b**) and UV-ozone exposure (**Figure 6c**). All the SH samples showed poor mechanical resistance, because they lose their water repellency properties after 2 cycles.

Concerning the UV-ozone test, we noted that the polytetrafluoroethylene coating remained unaltered after several cycles, while the rest of the surfaces were clearly damaged by at least one of these wear agents. All the surfaces showed a good resistance to prolonged water exposure (without change in their sliding angles). Due to their irrelevance, these results are not shown here.

The first anti-icing test conducted was the subcooled water repellency test. We observed that all the SH surfaces behaved very efficiently, avoiding ice accretion after subcooled water dripping for more than 12 hours. These results are drastically different than those ones obtained for the uncoated aluminum sample, for which the ice accretion occurred only 180 s after the beginning of the dripping process. The smooth-hydrophobic aluminum surface showed better results than the uncoated sample, but still much worse than the SH surfaces (ice accretion after 3 h).

Concerning the freezing delay tests, we could not observe remarkable differences between the three SH surfaces used in this study. However, we found important differences between the SH surfaces and the smooth (hydrophobized and uncoated) surfaces. Under dry conditions (low RH), the surface that delays freezing longer is the smooth-uncoated aluminum surface (**Figure 7a**), while at humid conditions (high RH), the SH surfaces delay freezing more efficiently than the smooth one (**Figure 7b**).

Results for the ice adhesion tests are shown in **Figure 8**. They show that the SH surfaces are unable to reduce shear (**Figure 8a**) and tensile ice adhesion (**Figure 8b**). Ice adhesion for the Ce-SA coating was clearly higher than the rest. These results reveal that the roughness enhances the ice adhesion.

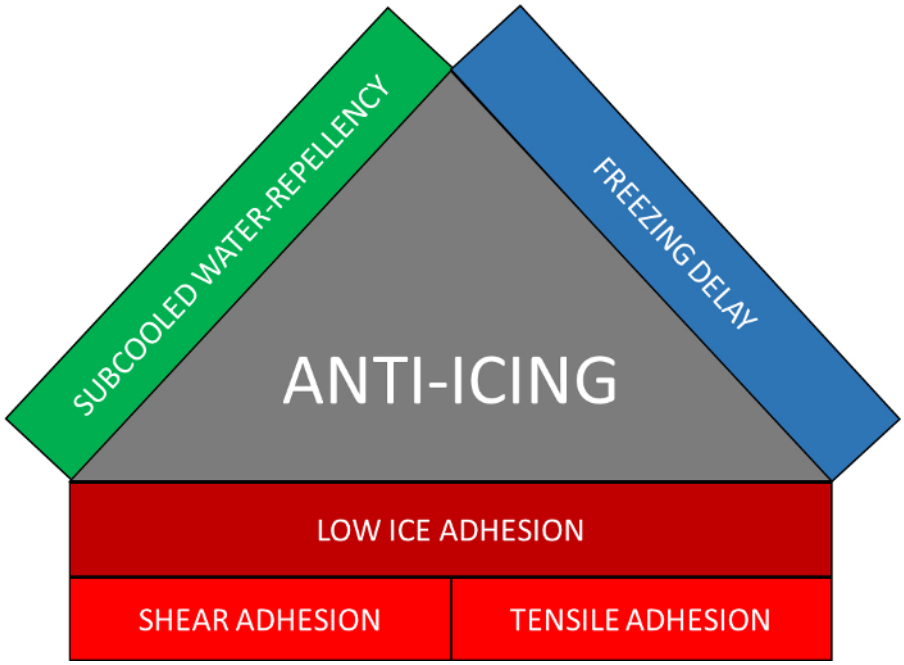

Figure 1. Three facets needed for anti-icing performance. Subcooled water repellency, freezing delay, and low shear/tensile ice adhesion.
Please click here to view a larger version of this figure.

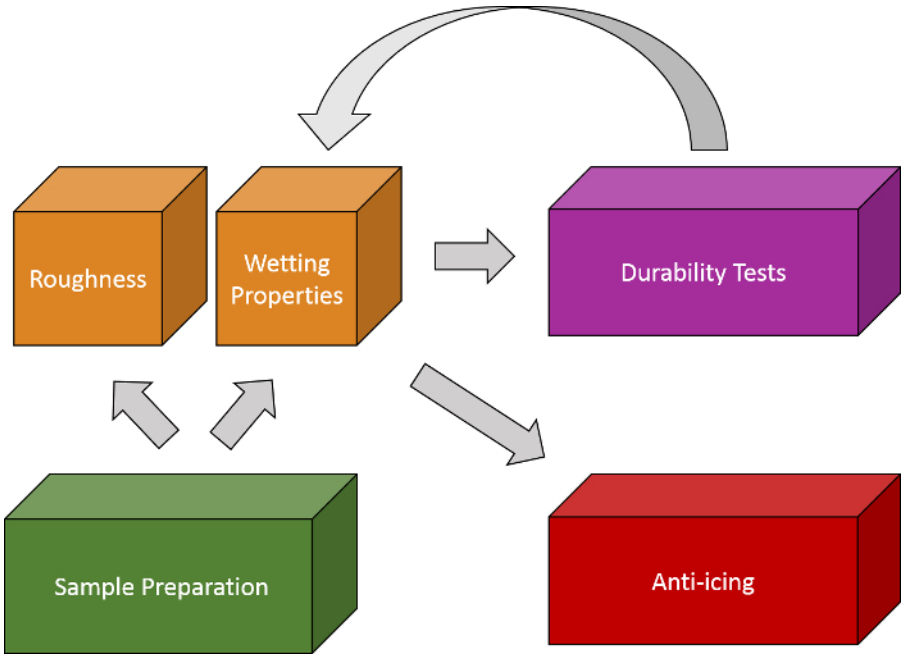

Figure 2. Scheme of the protocol followed in this work to fabricate and analyze the performance of superhydrophobic surfaces. First, the surfaces are prepared. Second, their wetting and roughness properties are analyzed, next durability, and, finally, their anti-icing efficiency.
Please click here to view a larger version of this figure.

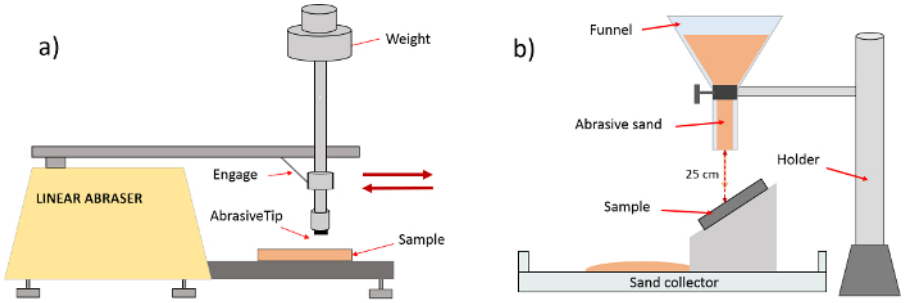

Figure 3. Mechanical durability tests. (a) Lateral abrasion test. **(b)** Particle impact test (erosion). Please click here to view a larger version of this figure.

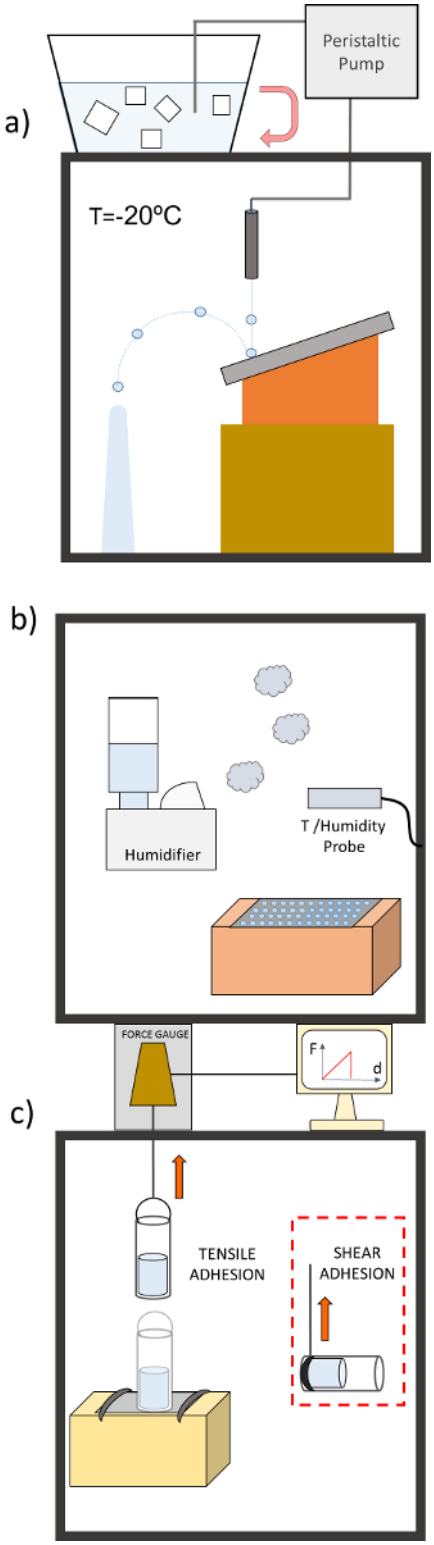

Figure 4. Anti-icing performance tests. **(a)** Subcooled water dripping test. **(b)** Freezing delay test. **(c)** Ice adhesion test Please click here to view a larger version of this figure.

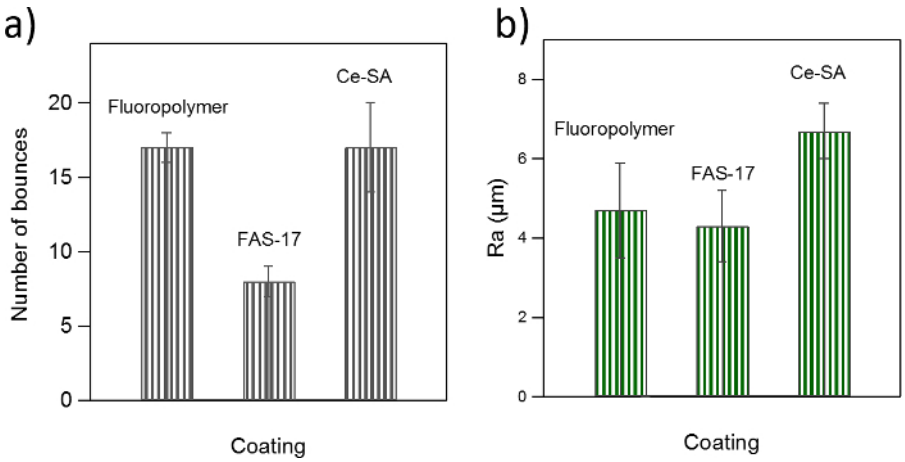

Figure 5. Water tensile adhesion and roughness properties of the superhydrophobic surfaces fabricated for this study. The water tensile adhesion is parametrized by **(a)** the number of bounces of a 4 µL water drop released over the sample and **(b)** the roughness by the roughness amplitude Ra. Error bars in (a) and (b) show the variability (standard deviation) within the same sample after conducting 3 bouncing drop experiments and after acquiring at least 4 single topographies, respectively. Please click here to view a larger version of this figure.

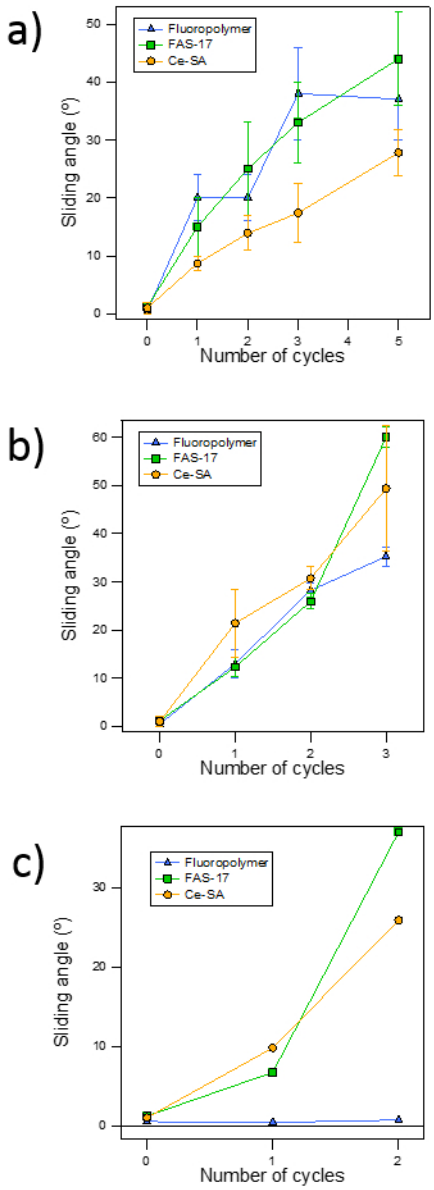

Figure 6. Sliding angle versus the number of cycles for each durability test. (a) Lateral abrasion test. **(b)** Particle impact. **(c)** UV-ozone. The error bars show the variability (standard deviation) after studying the dynamic of three sliding drops on each sample and for each wear condition.

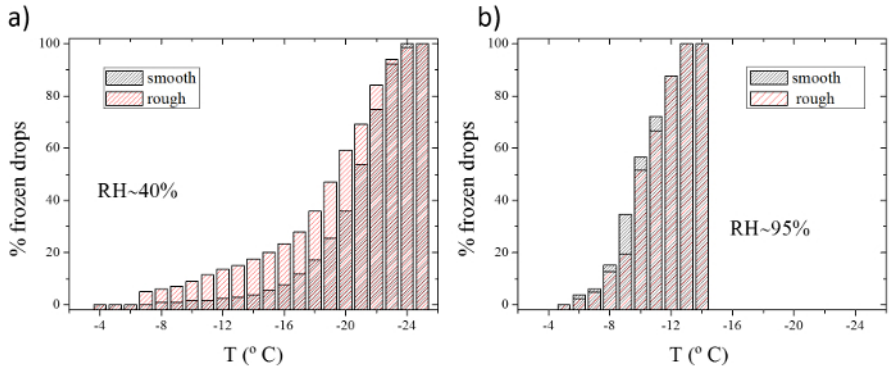

Figure 7. Freezing delay tests. Tests were conducted on a smooth-hydrophobic aluminum surface (fluoropolymer film coated) and a superhydrophobic surface (etched and fluoropolymer film coated) at (a) dry conditions (RH~40%) and (b) humid conditions (RH~95%). Please click here to view a larger version of this figure.

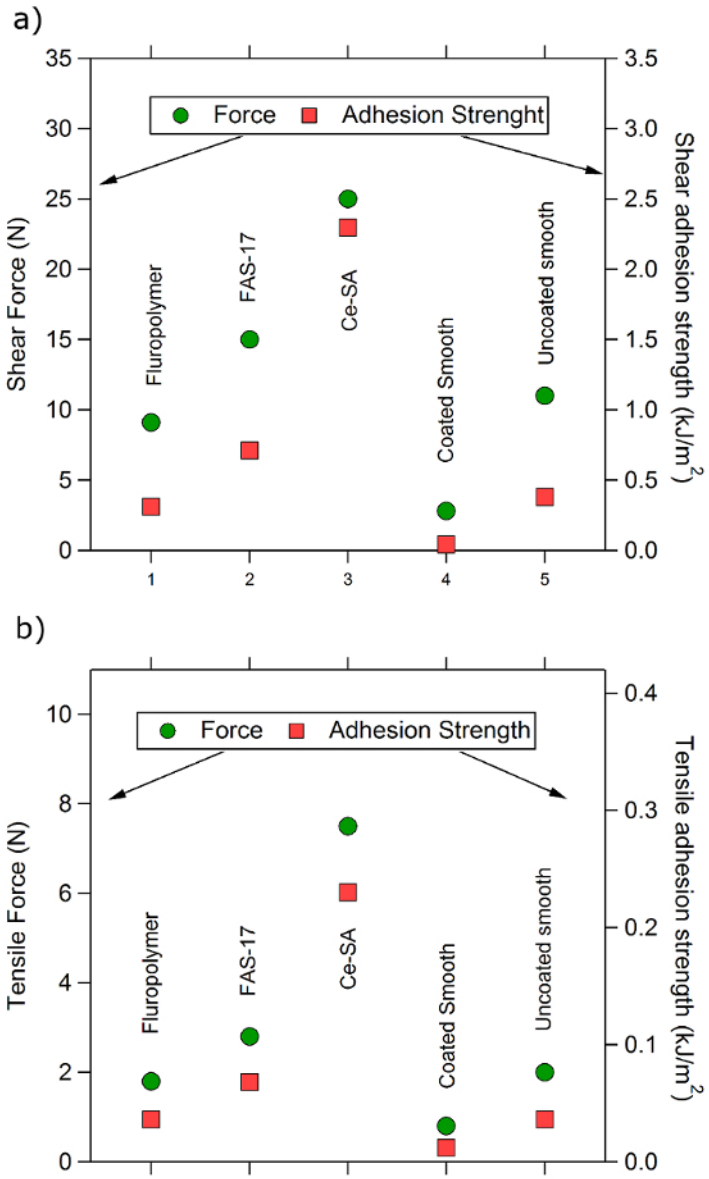

Figure 8. Ice adhesion quantified by peak force and adhesion strength. (a) Shear-adhesion tests. **(b)** Tensile adhesion tests. We studied the three superhydrophobic surfaces of this study and further analyzed a smooth-hydrophobized (fluoropolymer film coated) aluminum sample and an untreated aluminum sample, for comparison. Please click here to view a larger version of this figure.

Discussion

In this paper, we demonstrate strategies to produce water-repellent surfaces on aluminum substrates. In addition, we show methods to characterize their wetting properties, roughness, durability and anti-icing performance.

To prepare the SH surfaces, we used two strategies. The first strategy incorporated the proper roughness degree to achieve the intrinsic hierarchical structure of SH surfaces by acid etching. This process is particularly critical, which may require further work for other metals or aluminum substrates with different composition. Searching for the proper etching conditions may be an issue and typically requires a scanning of the etching time or acid concentrations. Acid etching is limited only to metal surfaces that are soluble in acid solutions or uncoated surfaces. In this work, we etched the substrate in HCl and later hydrophobized it with a fluoropolymer coating deposition or silanization (FAS-17), accordingly. The second strategy used a ceria coating that incorporates the roughness properties. This coating was deposited by immersion of the etched Al substrate.

The wetting response of the three coatings was examined with bouncing drop experiments. This technique is a significant improvement with respect to existing techniques for analyzing the wetting properties of superhydrophobic surfaces. The higher water repellency was obtained for the surfaces coated with fluoropolymer and Ce-SA, while the lowest repellency was achieved with FAS-17. The roughness degree of both the polytetrafluoroethylene and FAS-17 samples (Ra~4 μm) is very similar because the texturization protocol was the same. However, we expect a higher degree of coverage for the polytetrafluoroethylene coated sample, as confirmed in a previous study[13]. The sample coated with Ce-SA was

the roughest, but its water repellency was comparable to the polytetrafluoroethylene samples. This suggests that roughness in not necessary beneficial above a certain degree or roughness. The three SH surfaces showed poor mechanical durability. The Ce-SA samples showed a remarkably better resistance to shear abrasion than the rest (**Figure 6a**). Otherwise, all the SH surfaces showed very similar degradation after the sand-abrasion wear test. The surface coated with polytetrafluoroethylene resisted the UV-ozone wear test very efficiently. This might be connected to the high chemical stability of polytetrafluoroethylene[36]. All the SH surfaces showed good resistance to prolonged water exposure. Concerning the anti-icing performance, we concluded that the SH surfaces are very efficient as a subcooled water repellent, since no ice accretion was observed after more than 12 hours under constant water-dripping and further as freezing delayers at humid conditions (**Figure 7b**). This observation is in good agreement with previous results[24]. However, the ice adhesion tests revealed an unsatisfactory performance of the SH surfaces in comparison to the control smooth samples used for this test (uncoated and hydrophobized). Our results confirmed that the roughness enhances noticeably the ice adhesion (**Figure 8**), which is in good agreement with previous observations[26]. Affecting subcooled water and high humidity are environmental conditions typical for icing. However, if ice is inexorably formed on the surface, the ice removal from SH surfaces might be a very difficult task. Other alternatives (elastomeric coatings or slippery surfaces, for instance) that are not superhydrophobic surfaces are proposed for anti-icing applications. The techniques presented in this work to evaluate both the durability and anti-icing properties may be similarly used to compare the anti-icing efficiency of these surfaces.

Disclosures

We have nothing to disclose.

Acknowledgements

This research was supported by the projects: MAT2014-60615-R and MAT2017-82182-R funded by the State Research Agency (SRA) and European Regional Development Fund (ERDF).

References

1. Fang, G., & Amirfazli, A. Understanding the anti-icing behavior of superhydrophobic surfaces. *Surface Innovations.* **2** (2), 94-102 (2014).
2. Wang, N. *et al.* Robust superhydrophobic coating and the anti-icing properties of its lubricants-infused-composite surface under condensing condition. *New Journal of Chemistry.* **41** (4), 1846-1853 (2017).
3. Jung, S. *et al.* Are superhydrophobic surfaces best for icephobicity? *Langmuir.* **27** (6), 3059-3066 (2011).
4. Milionis, A., Loth, E., & Bayer, I. S. Recent advances in the mechanical durability of superhydrophobic materials. *Advances in Colloid and Interface Science.* **229** 57-79 (2016).
5. Li, X.-M., Reinhoudt, D., & Crego-Calama, M. What do we need for a superhydrophobic surface? A review on the recent progress in the preparation of superhydrophobic surfaces. *Chemical Society Reviews.* **36** (8), 1350-1368 (2007).
6. Sun, M. *et al.* Artificial Lotus Leaf by Nanocasting. *Langmuir.* **21** (19), 8978-8981 (2005).
7. Darmanin, T., & Guittard, F. Superhydrophobic and superoleophobic properties in nature. *Materials Today.* **18** (5), 273-285 (2015).
8. Marmur, A. Soft contact: Measurement and interpretation of contact angles. *Soft Matter.* **2** (1), 12-17 (2006).
9. Li, W., & Amirfazli, A. Hierarchical structures for natural superhydrophobic surfaces. *Soft Matter.* **4** (3), 462-466 (2008).
10. Ruiz-Cabello, F. J. M., Rodríguez-Criado, J. C., Cabrerizo-Vílchez, M., Rodríguez-Valverde, M. A., & Guerrero-Vacas, G. Towards super-nonstick aluminized steel surfaces. *Progress in Organic Coatings.* **109**, 135-143 (2017).
11. Yuan, Z. *et al.* Fabrication of superhydrophobic surface with hierarchical multi-scale structure on copper foil. *Surface and Coatings Technology.* **254**, 151-156 (2014).
12. Varshney, P., Mohapatra, S. S., & Kumar, A. Superhydrophobic coatings for aluminium surfaces synthesized by chemical etching process. *International Journal of Smart and Nano Materials.* **7** (4), 248-264 (2016).
13. Ruiz-Cabello, F. J. M. *et al.* Testing the performance of superhydrophobic aluminum surfaces. *Journal of Colloid and Interface Science.* **508**, 129-136 (2017).
14. Mahadik, S. A. *et al.* Superhydrophobic silica coating by dip coating method. *Applied Surface Science.* **277**, 67-72 (2013).
15. Xu, L., Karunakaran, R. G., Guo, J., & Yang, S. Transparent, superhydrophobic surfaces from one-step spin coating of hydrophobic nanoparticles. *ACS Applied Materials & Interfaces.* **4** (2), 1118-1125 (2012).
16. Montes Ruiz-Cabello, F. J., Amirfazli, A., Cabrerizo-Vilchez, M., & Rodriguez-Valverde, M. A. Fabrication of water-repellent surfaces on galvanized steel. *RSC Advances.* **6** (76), 71970-71976 (2016).
17. Li, L., Breedveld, V., & Hess, D. W. Creation of superhydrophobic stainless steel surfaces by acid treatments and hydrophobic film deposition. *ACS Applied Materials & Interfaces.* **4** (9), 4549-4556 (2012).
18. Wang, N., Xiong, D., Deng, Y., Shi, Y., & Wang, K. Mechanically robust superhydrophobic steel surface with anti-icing, UV-durability, and corrosion resistance properties. *ACS Applied Materials & Interfaces.* **7** (11), 6260-6272 (2015).
19. Azimi, G., Kwon, H.-M., & Varanasi, K. K. Superhydrophobic surfaces by laser ablation of rare-earth oxide ceramics. *MRS Communications.* **4** (3), 95-99 (2014).
20. Liang, J., Hu, Y., Fan, Y., & Chen, H. Formation of superhydrophobic cerium oxide surfaces on aluminum substrate and its corrosion resistance properties. *Surface and Interface Analysis.* **45** (8), 1211-1216 (2013).
21. Azimi, G., Dhiman, R., Kwon, H.-M., Paxson, A. T., & Varanasi, K. K. Hydrophobicity of rare-earth oxide ceramics. *Nature Materials.* **12**, 315 (2013).
22. Ruan, M. *et al.* Preparation and anti-icing behavior of superhydrophobic surfaces on aluminum alloy substrates. *Langmuir.* **29** (27), 8482-8491 (2013).
23. Yin, L. *et al.* In situ investigation of ice formation on surfaces with representative wettability. *Applied Surface Science.* **256** (22), 6764-6769 (2010).
24. Boinovich, L., Emelyanenko, A. M., Korolev, V. V., & Pashinin, A. S. Effect of wettability on sessile drop freezing: when superhydrophobicity stimulates an extreme freezing delay. *Langmuir.* **30** (6), 1659-1668 (2014).

25. Antonini, C., Innocenti, M., Horn, T., Marengo, M., & Amirfazli, A. Understanding the effect of superhydrophobic coatings on energy reduction in anti-icing systems. *Cold Regions Science and Technology.* **67** (1-2), 58-67 (2011).
26. Chen, J. *et al.* Superhydrophobic surfaces cannot reduce ice adhesion. *Applied Physics Letters.* **101** (11), 111603 (2012).
27. Adam, S., Barada, K. N., Alexander, D., Mool, C. G., & Eric, L. Linear abrasion of a titanium superhydrophobic surface prepared by ultrafast laser microtexturing. *Journal of Micromechanics and Microengineering.* **23** (11), 115012 (2013).
28. Li, X.-W. *et al.* Low-cost and large-scale fabrication of a superhydrophobic 5052 aluminum alloy surface with enhanced corrosion resistance. *RSC Advances.* **5** (38), 29639-29646 (2015).
29. Meuler, A. J. *et al.* Relationships between water wettability and ice adhesion. *ACS Applied Materials & Interfaces.* **2** (11), 3100-3110 (2010).
30. Boinovich, L. B. *et al.* Combination of functional nanoengineering and nanosecond laser texturing for design of superhydrophobic aluminum alloy with exceptional mechanical and chemical properties. *ACS Nano.* **11** (10), 10113-10123 (2017).
31. Wan, B. *et al.* Superhydrophobic ceria on aluminum and its corrosion resistance. *Surface and Interface Analysis.* **48** (3), 173-178 (2016).
32. Gómez-Lopera, J. F., Martínez-Aroza, J., Rodríguez-Valverde, M. A., Cabrerizo-Vílchez, M. A., & Montes-Ruíz-Cabello, F. J. Entropic image segmentation of sessile drops over patterned acetate. *Mathematics and Computers in Simulation.* **118**, 239-247 (2015).
33. Gao, L., & McCarthy, T. J. Teflon is hydrophilic. comments on definitions of hydrophobic, shear versus tensile hydrophobicity, and wettability characterization. *Langmuir.* **24** (17), 9183-9188 (2008).
34. Ruiz-Cabello, F. J. M., Rodriguez-Valverde, M. A., & Cabrerizo-Vilchez, M. A new method for evaluating the most stable contact angle using tilting plate experiments. *Soft Matter.* **7** (21), 10457-10461 (2011).
35. Pierce, E., Carmona, F. J., & Amirfazli, A. Understanding of sliding and contact angle results in tilted plate experiments. *Colloids Surfaces A.* **323** (1-3), 73-82 (2008).
36. Ye, H., Zhu, L., Li, W., Liu, H., & Chen, H. Simple spray deposition of a water-based superhydrophobic coating with high stability for flexible applications. *Journal of Materials Chemistry.* **5** (20), 9882-9890 (2017).
37. Rolland, J. P., Van Dam, R. M., Schorzman, D. A., Quake, S. R., & DeSimone, J. M. Solvent-resistant photocurable "liquid Teflon" for microfluidic device fabrication. *Journal of the American Chemical Society.* **126** (8), 2322-2323 (2004).

